




Division of Labor, Bet Hedging, and the Evolution of Mixed Biofilm Investment Strategies

 Nick Vallespir Lowery,^{a*} Luke McNally,^{a,b} William C. Ratcliff,^c Sam P. Brown^{a,b,c}

Institute of Evolutionary Biology, School of the Biological Sciences, University of Edinburgh, Edinburgh, United Kingdom^a; Centre for Immunity, Infection and Evolution, School of the Biological Sciences, University of Edinburgh, Edinburgh, United Kingdom^b; School of Biology, Georgia Institute of Technology, Atlanta, Georgia^c

ABSTRACT Bacterial cells, like many other organisms, face a tradeoff between longevity and fecundity. Planktonic cells are fast growing and fragile, while biofilm cells are often slower growing but stress resistant. Here we ask why bacterial lineages invest simultaneously in both fast- and slow-growing types. We develop a population dynamic model of lineage expansion across a patchy environment and find that mixed investment is favored across a broad range of environmental conditions, even when transmission is entirely via biofilm cells. This mixed strategy is favored because of a division of labor where exponentially dividing planktonic cells can act as an engine for the production of future biofilm cells, which grow more slowly. We use experimental evolution to test our predictions and show that phenotypic heterogeneity is persistent even under selection for purely planktonic or purely biofilm transmission. Furthermore, simulations suggest that maintenance of a biofilm subpopulation serves as a cost-effective hedge against environmental uncertainty, which is also consistent with our experimental findings.

IMPORTANCE Cell types specialized for survival have been observed and described within clonal bacterial populations for decades, but why are these specialists continually produced under benign conditions when such investment comes at a high reproductive cost? Conversely, when survival becomes an imperative, does it ever benefit the population to maintain a pool of rapidly growing but vulnerable planktonic cells? Using a combination of mathematical modeling, simulations, and experiments, we find that mixed investment strategies are favored over a broad range of environmental conditions and rely on a division of labor between cell types, where reproductive specialists amplify survival specialists, which can be transmitted through the environment with a limited mortality rate. We also show that survival specialists benefit rapidly growing populations by serving as a hedge against unpredictable changes in the environment. These results help to clarify the general evolutionary and ecological forces that can generate and maintain diverse subtypes within clonal bacterial populations.

KEYWORDS biofilms, evolution, microbial ecology

After billions of years of evolution, many organisms retain an impressive capacity for innovation and adaptation to their environment. However, for core traits such as durability and the reproductive rate, improvements in one will often come at the cost of another—indeed, understanding how adaptation occurs when key fitness parameters are constrained by tradeoffs lies at the core of life history theory (1). While most life history theory has been developed with large multicellular organisms in mind, microbes also exhibit classical trade-offs in fecundity and longevity, with faster-growing lineages tending to be more fragile (2, 3). Understanding how microbes manage such trade-offs remains a major goal in microbiology from both mechanistic (4) and ecological (5) perspectives.

Received 31 May 2017 **Accepted** 28 June 2017 **Published** 8 August 2017

Citation Lowery NV, McNally L, Ratcliff WC, Brown SP. 2017. Division of labor, bet hedging, and the evolution of mixed biofilm investment strategies. *mBio* 8:e00672-17. <https://doi.org/10.1128/mBio.00672-17>.

Editor Matthew R. Parsek, University of Washington

Copyright © 2017 Lowery et al. This is an open-access article distributed under the terms of the [Creative Commons Attribution 4.0 International license](https://creativecommons.org/licenses/by/4.0/).

Address correspondence to Nick Vallespir Lowery, nlowery@uoregon.edu, or Sam P. Brown, sam.brown@biology.gatech.edu.

* Present address: Nick Vallespir Lowery, META Center for Systems Biology, University of Oregon, Eugene, Oregon, USA.

Multiple mechanisms for enhancing durability and longevity are available to microbes but typically come at the cost of reduced metabolic proficiency. Spore formation is perhaps the clearest example of a high-survival, low-fecundity phenotype; by encasing the genome and some essential metabolic machinery in a thick and extremely resistant cell wall, dormant spores can survive for extraordinarily long durations (6, 7). Alternatively, cells may form metabolically dormant persister cells capable of surviving diverse environmental insults (8, 9). Finally, many microbial species form biofilms where dense cell packing and production of a protective extracellular matrix provide broad resistance to stressors such as desiccation, predation, or chemical insult (10) but also limit space and nutrient diffusion, thereby reducing growth rates.

Clonally reproducing microbes present an interesting and experimentally tractable system in which to examine mixed behavioral strategies. Across many species of microbes, single genotypes can produce coexisting subpopulations of rapidly dividing planktonic cells and slow-growing or dormant stress-tolerant phenotypes, but focus is often given to a specific phenotype of interest rather than the balance between alternate phenotypes. In this study, we examined how the trade-off between the survival and growth of individual cells drives the evolution of mixed biofilm/planktonic investments on a lineage scale under diverse environmental conditions. Specifically, we build population dynamic models of bacteria in patchy environments where cells can switch between biofilm and planktonic states within ephemeral patches (via planktonic colonization of the biofilm and dispersal from the biofilm to the planktonic state) and can also be transmitted among patches as either biofilm or planktonic cells. We then ask under what conditions investment in biofilm is favored, given that biofilms grow more slowly. If only one phenotype (i.e., biofilm or planktonic) is favored for transmission to a new patch, does it ever pay to diversify into the cell type that is, from a transmission perspective, a dead end? Our model predicts that phenotypic diversification can pay across a wide range of environmental conditions, as rapidly growing planktonic cells can function as a “growth engine” providing higher levels of future planktonic and biofilm cells for transmission. We then test our model predictions by using stochastic simulations and experimental evolution of biofilm allocation in the environmental microbe *Pseudomonas aeruginosa*.

RESULTS

Biofilm growth dynamics. While it is well known that planktonic cells accumulate exponentially in nutrient-rich environments, it is less clear whether close-packed biofilm cells would follow the same functional form (note that here we are considering biofilm growth in the absence of any coupling with the planktonic compartment, i.e., no cells dispersing from the biofilm or colonizing from the bulk). We hypothesize that sparse colonization allows for lineages to grow exponentially, as there is little steric inhibition or nutrient depletion to slow growth. However, once confluence across the surface is reached, further growth is restricted to a fixed depth within the outermost layer in biofilms because of space and diffusion limitations (11, 12). We explore this conjecture by using the individual-based simulation platform iDyNoMiCS (13) to simulate a simple two-dimensional (2D) biofilm and find that after an initial period of exponential growth, cell accumulation decays to a linear function in time (Fig. 1). More generally, we find that the rate of biofilm growth depends on the geometry of the system being considered (see Text S1 in the supplemental material), with the growth rate following a polynomial of order equal to the dimensionality of the system (i.e., for a 3D sphere, biofilm cells accumulate as a cubic in time). However, it should be noted that for finite volumes, there is a constant downward pressure through time on the order of the growth polynomial as the biofilm reaches confluence across each dimension (e.g., initially cubic expansion in three dimensions will decay to quadratic expansion in two dimensions once the limit in the *z* direction is reached). These findings highlight that while biofilm cells do not face the extreme growth penalty of resistant spores or persister cells, they face a significant and compounding growth deficit in comparison with the exponential growth of planktonic populations.

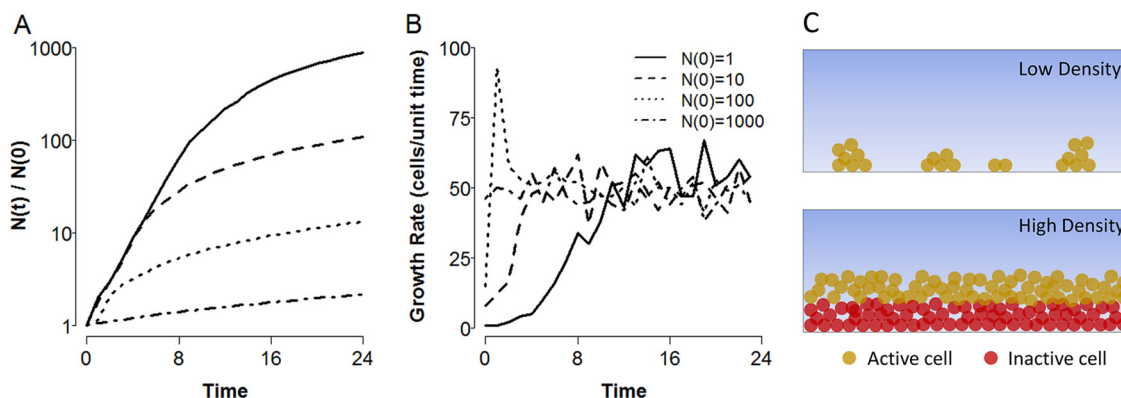


FIG 1 Biofilms grow subexponentially. (A, B) Numbers of accumulated cells (A) and lineage growth rates (B) through time for agent-based simulations of a 2D biofilm growing on a 1D surface. Various inocula (see inset) were allowed to grow for a fixed time period under nutrient-rich conditions. Simulations were implemented with the agent-based simulation platform iDynoMICS (13). (C) Schematic depiction of nutrient depletion leading to growth arrest in the biofilm interior. Diffusion and active consumption of nutrients in the outermost layers of the biofilm (yellow cells) result in starvation conditions for cells in the interior regions (red cells).

Coupled biofilm-plankton dynamics. We next model a growing bacterial microcosm within which cells grow in one of two compartments, the planktonic (P) phase within the bulk fluid and the biofilm (B) phase attached to a surface and in contact with the bulk. The compartments are coupled such that biofilm cells can disperse to the planktonic phase and planktonic cells can colonize the biofilm. Cells in each compartment also divide, with planktonic cells growing exponentially and biofilm cells growing linearly (i.e., we assume a finite 2D surface available for biofilm colonization and ignore the initial superlinear growth period).

With the biofilm limited to linear expansion, we reasoned that the effects of growth within and dispersal from the biofilm would be negligible when coupled to exponential growth in the planktonic phase. This simplification was shown to be reasonable by comparing numerical simulations of the full model and a simplified model with no biofilm growth or dispersal (Fig. S1), yielding the model system outlined in equations 1 to 4 for within-patch growth. By setting the growth of the biofilm to zero, this simplified framework renders biofilm cells functionally equivalent to spores or persisters as described above, i.e., a subpopulation of nondividing cells supported by the growth of vegetative cells, which presumably must provide some other benefit (e.g., environmental resistance) to the overall population to counteract this loss of fitness or else be lost from the population.

Our simplified model framework results in the following coupled differential equations:

$$\frac{dP}{dt} = (r - c)P \tag{1}$$

$$\frac{dB}{dt} = cP \tag{2}$$

where B and P are the numbers of biofilm and planktonic cells, respectively, r is the exponential growth rate, and c is the rate of colonization of the biofilm (with $0 \leq c < r$). Note that, in general, c need not be bounded by r and arbitrarily high values of c would result in a decline in P as switching to the biofilm phase outpaces planktonic growth, giving a sharp trade-off between the two compartments; we discuss this case in the context in which it arises below. Solving equations 1 and 2 as a function of time yields our within-patch population model as follows:

$$P(t) = P_0 e^{(r-c)t} \tag{3}$$

$$B(t) = \frac{c}{r - c} [P(t) - P_0] \tag{4}$$

where P_0 is the planktonic inoculum.

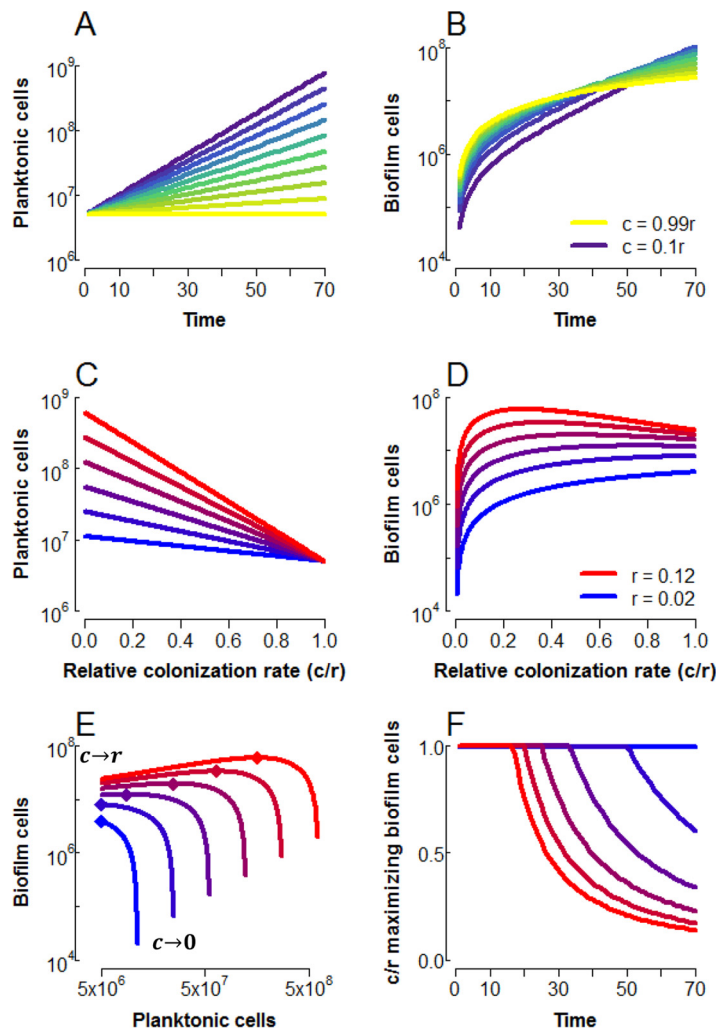


FIG 2 Maximal biofilm can be driven by planktonic growth. (A, B) Time series of planktonic (A) and biofilm (B) cells for colonization rates (c values) between $0.1 r$ (purple) and $0.99 r$ (yellow), with $r = 0.08$, $P_0 = 5,000,000$. (C, D) Planktonic (C) and biofilm (D) cells as a function of colonization rate relative to growth rate for $t = 40$, $0.02 \leq r \leq 0.12$ (blue-red color scale), $P_0 = 5,000,000$. (E) Biofilm cells plotted against planktonic cells under the same conditions as in panels C and D. The colonization rate varies over each curve, with the endpoints indicated by labels (the relative colonization rate, c/r , approaches 1 at the left and zero at the right). Diamonds indicate the maximum in biofilm cells. (F) Relative colonization rate, c/r , at which biofilm is maximized. Note that in panels D and E, the limit of $c = 0$ is omitted, as this prevents any formation of biofilm cells.

The within-patch model reveals a temporal trade-off in biofilm accumulation with increasing colonization (Fig. 2). As expected, planktonic cells decline monotonically with an increasing colonization rate, c , as more cells are siphoned from the planktonic to the biofilm compartment (Fig. 2A and C). The biofilm, however, shows more interesting dynamics with changing rates of colonization (Fig. 2B and D). At $c = 0$, no biofilm cells accumulate, and as c approaches r , all new planktonic cells colonize the biofilm, resulting in a static planktonic population and linear accumulation of biofilm cells (Fig. 2A and B, yellow lines). However, when the planktonic fraction is allowed to expand exponentially (with $0 < c < r$), the biofilm also accumulates cells roughly exponentially [once $P(t) \gg P_0$] at a constant fraction $c/(r - c)$ of the planktonic population. High colonization rates thus provide more biofilm cells at short time scales, while lower colonization rates maximize biofilm over longer periods of growth (Fig. 2B).

As shown in Fig. 2D, we find that the colonization rate maximizing biofilm cells declines with increasing planktonic growth rates, giving a humped shape in biofilm as

a function of the colonization rate. We can find an analytical condition for this relationship by examining the slope of B as a function of c as c approaches r (see Text S2 for derivation) as follows:

$$\lim_{c \rightarrow r} \left(\frac{dB}{dc} \right) = -\frac{1}{2} P_0 t (rt - 2) \quad (5)$$

If the slope is negative, this would imply an interior maximum in B at some value of c that is $< r$ (as biofilm cells necessarily increase as c increases from zero). We find that this limit is negative when the product of rt is > 2 ; i.e., the presence of a humped relationship in B requires patch quality (the product of rt) to exceed a minimal threshold value.

These results suggest that the colonization rate maximizing biofilm will depend on opportunities for growth in the planktonic state (governed by growth rate r and growth duration t), which we explore further in Fig. 2E and F. In Fig. 2E, plotting biofilm cells against planktonic cells reveals that while limited growth (blue lines) leads to an allocation trade-off (i.e., increasing B necessarily comes at the cost of decreasing P), an increasing growth rate decouples this trade-off, with B maximized at diminishing colonization rates c , depicted explicitly in Fig. 2F. However, as colonization decreases beyond this point, biofilm declines sharply as colonization tends to zero.

Under high growth regimes, the planktonic fraction may therefore be viewed as a “growth engine” to maximize biofilm; when within-patch conditions are sufficiently favorable to planktonic division (equation 5), reducing the biofilm colonization rate, c , below the maximum increases the net flux of cells into the biofilm by expanding the pool of dividing planktonic cells, P . This growth engine effect is sufficient to drive colonization rates maximizing biofilm down to a fraction of the growth rate (Fig. 2F).

Evolutionary model. While intermediate colonization rates may maximize biofilm, we note that any allocation toward the biofilm comes at the cost of total population size (as shown in equation 6)

$$\frac{d[P(t) + B(t)]}{dc} = -\frac{rP_0\{1 + [(r - c)t - 1]e^{(r-c)t}\}}{(r - c)^2} \quad (6)$$

which is strictly negative when t is > 0 and equal to 0 when t equals 0. Given this trade-off between the biofilm and total population size, what conditions would favor biofilm investment (c of > 0)? We can examine the evolutionary consequences of allocation in the within-patch population model by constructing a life cycle in which a population colonizes successive patches through space and/or time (i.e., migration between patches or remaining in a single patch that experiences periodic disturbances). We define a fitness function by assigning transmission probabilities k_p and k_b that a given cell from the respective planktonic or biofilm compartment will go on to found a new patch as follows:

$$W = k_p P(t) + k_b B(t) \quad (7)$$

or, explicitly, per founding cell (analogous to the reproductive number “R0” framework common to parasite epidemiology and evolution [14]) as follows:

$$W(c, r, t) = k_p e^{(r-c)t} + k_b [e^{(r-c)t} - 1] \frac{c}{r - c} \quad (8)$$

Equation 8 allows us to interrogate the fitness consequences of biofilm investment strategies (colonization rate c) across a wide array of ecological parameters. k_p and k_b capture the reproductive value of each cell type and can be interpreted equivalently as a per-cell transmission probability or as the fraction of each subpopulation able to be transmitted successfully; they will dictate how well a given cell type (biofilm or planktonic) can survive the interpatch transition and be influenced by the nature of the environment. Growth time t describes the disturbance regime, i.e., how long a population can stay in a single patch, and r measures the nutrient quality of individual patches or how rapidly planktonic cells can divide within the patch. We define c^* as the optimal colonization rate maximizing fitness W under a given ecological condition and display the behavior of c^* as a function of transmission parameters k_p and k_b in Fig. 3.

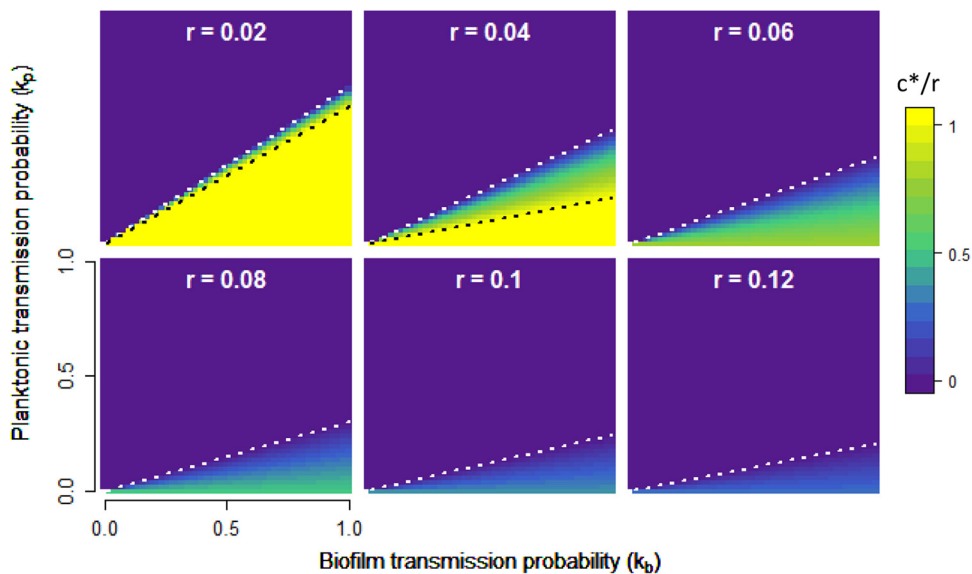


FIG 3 Optimal colonization rate, c^* , as a function of the reproductive value of planktonic and biofilm cells. Contour plots show the relative colonization rate (c^*/r , yellow-purple color scale) optimizing fitness (equation 8). Each panel displays c^*/r as a function of k_p and k_b . Across panels, the growth rate, r , increases from 0.02 to 0.12, with $t = 40$ in all cases; similar plots varying t are displayed in Fig. S2. A white dotted line indicates the point at which c^* transitions from 0 to >0 , while a black dotted line indicates the threshold at which c^* becomes 1 (see text and Text S3).

There are three general strategies microbes may adopt in maximizing fitness, devoting all resources to the biofilm fraction ($c^* = r$, below black dotted lines in Fig. 3), splitting resources between the two fractions ($0 < c^* < r$, between dotted lines in Fig. 3), and devoting all resources to the plankton ($c^* = 0$, above white dotted lines in Fig. 3). In Text S3, we investigate the conditions governing the two transitions defining these regimes by examining the behavior of equation 8 in more detail.

Trade-offs in allocation. When growth opportunities are limited (Fig. 3, upper left panel), we see evidence of a sharp tradeoff between B and P investment, with very little parameter space allowing intermediate investments ($0 < c^* < r$). In the limit of zero within-patch growth, the allocation decision becomes a zero-sum game, with no allowance for intermediate investment, as follows:

$$\left. \frac{dW}{dc} \right|_{r=0} = te^{-ct}(k_b - k_p) \quad (9)$$

In this no-growth scenario ($r = 0$), if biofilm cells have greater transmission value ($k_b > k_p$), then total biofilm investment is favored; if not, then total planktonic cell investment is favored, giving a strict trade-off defined by whichever fraction is preferentially transmitted between patches.

This simple zero-sum logic is intuitive but fails significantly under more permissive growth conditions (i.e., increasing r and/or t ; Fig. 3; Fig. S2), where we see an intermediate level of colonization is favored over a relatively large portion of the parameter space. Despite large transmission advantages to biofilm cells, the intermediate colonization regime extends to the boundary of $k_p = 0$ (black dashed line undefined for $r > 0.04$, Fig. 3), such that even when planktonic cells have zero probability of founding a new patch, the vast majority of the population is still allocated to that fraction. This result follows from the dynamics of the within-patch model (equations 3 and 4; Fig. 2); when $k_p = 0$, fitness is determined entirely by the size of the biofilm population, which is maximized at low colonization rates under conditions favoring growth because of the driving force of the planktonic growth engine.

Biofilm as a hedge against environmental instability. In our evolutionary model (Fig. 3), we assume that lineages can adapt their allocation decision making (c^*) in the

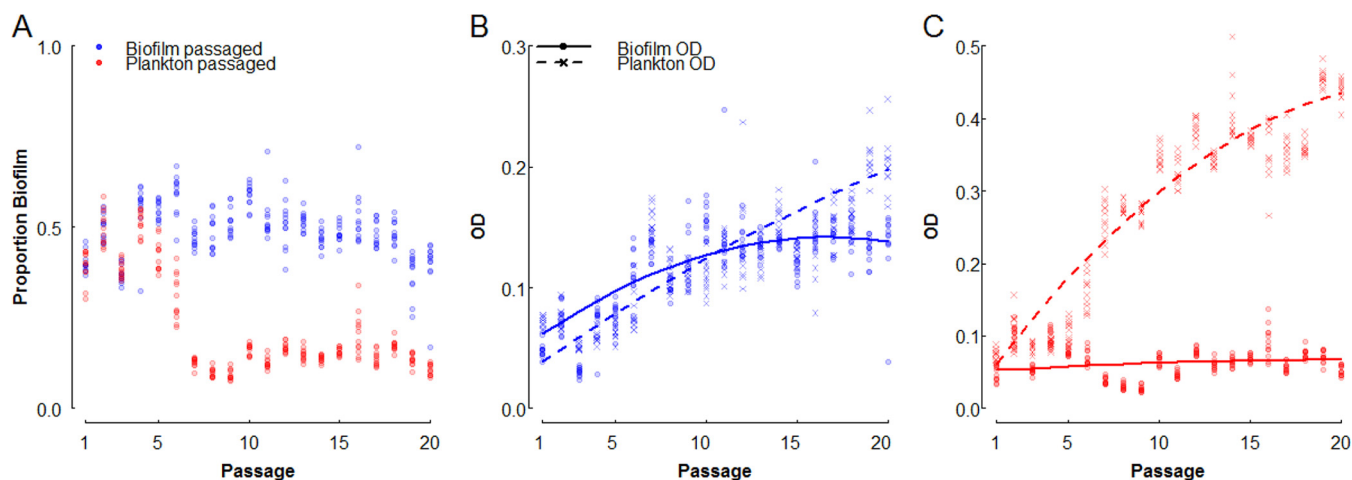


FIG 4 Selection experiments recapitulate model predictions. *P. aeruginosa* PAO1 was grown at room temperature in 96-well plates each well of which contained a glass bead, and every 12 h, populations were fractionated, measured, and passaged to a new well. Shown are the proportion of biofilm (defined as the ratio of the biofilm OD to the sum of the ODs of the two fractions) (A) and fractionated ODs of biofilm growth-selected ($k_b = 1, k_p = 0$) (B) and planktonic-growth-selected ($k_b = 0, k_p = 1$) (C) lines over the course of the passaging experiment. Points represent 12 independently evolving lineages per treatment, and curves show best-fit regression (adjusted $R^2 = 0.92$, Table S1). All reported ODs are corrected for the OD of the blank medium.

context of constant transmission weightings k_p and k_b . However, the relative success of biofilm versus planktonic cell propagules is likely to vary extensively in time as a function of unpredictable biotic and abiotic stresses (i.e., changing k_p relative to k_b). Despite reduced colonization rates leading to larger planktonic populations, sharply diminishing returns from further decreases in c (Fig. 2E) suggest that the biofilm compartment has the potential to function as a cost-effective hedge against unpredictable selective events. At all growth rates, populations can exchange a small reduction in the size of the planktonic population for a massive increase in the biofilm population by raising the rate of colonization from a minimal value; returning to equations 1 and 2, taking the ratio of the biofilm to the planktonic growth rate yields the fraction $c/(r - c)$, which approaches infinity as c approaches r .

Maintaining a small biofilm presence therefore has a relatively low cost, even in the absence of environmental stresses that favor biofilm cells, suggesting that selection against low rates of biofilm production will be weak. To test this hypothesis, we performed a selection experiment in which 12 replicate populations of *P. aeruginosa* were subjected to 20 transfers (approximately 130 generations), allowing only planktonic or only biofilm cells to survive (Fig. 4). While relative biofilm production rapidly decreased in the plankton-selected lines ($k_b = 0, k_p = 1$, red points in Fig. 4A), declining from ~40% to ~13% of the cells in biofilms after 7 transfers (paired t test, mean difference = 0.265, $t = 18.7$, $df = 11$, $P = 1.1 \times 10^{-9}$), biofilm production did not evolve to be any lower over the remaining 13 transfers of the experiment (Fig. 4A, biofilm fraction from passages 7 to 20 best fit by an intercept model [Akaike information criterion (AIC) = -580] versus a linear model [AIC = -424]; also note that in Fig. 4C, the biofilm optical density [OD] stays roughly constant over the course of the experiment).

Interestingly, in the biofilm-only selection line ($k_b = 1, k_p = 0$; Fig. 4A, blue points), the proportion of cells in biofilms did not increase over the course of the experiment, although the total number of cells in the biofilm increased by more than 100% (Fig. 4B). Particularly, we see that the planktonic cell density increases steadily while the biofilm fraction increases initially and then stagnates after roughly 10 passages (Fig. 4B; Table S1). We did not observe significant morphological or phenotypic diversification in these lines (Fig. S3), suggesting that evolution of planktonic or biofilm growth-specialized lineages (15, 16) was not a major driver of population dynamics. This result is consistent with our models above, with planktonic growth driving biofilm accumulation, and experimentally demonstrates the utility of a mixed strategy under strict selection regimes.

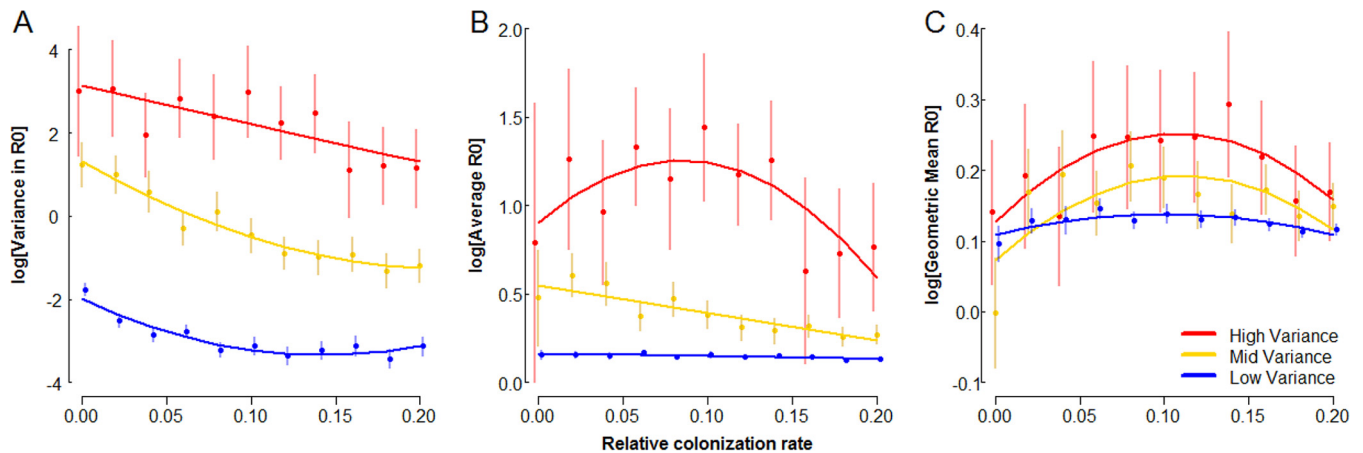


FIG 5 Biofilm production can act as a bet-hedging strategy. Shown are log-scale plots of variance in R0 (A), average R0 (B), and geometric mean R0 (C) as a function of the relative colonization rate (ratio of c to the expected value of r ; see below) for lineages subjected to passing simulations with different levels of environmental instability. One hundred replicate inocula of 5,000 planktonic cells with the same fixed colonization rates, $c \in (0, 0.2)$, were subjected to 10 passages. In all cases, $\mu_r = 0.06$, $\mu_t = 40$, $\mu_{k_p} = 0.1$, and $\mu_{k_b} = 0.6$. Under fixed conditions, these parameters would favor a c^* of 0.49. Variance treatments modified the σ^2 of the distributions from which r , t , k_p , and k_b were drawn, with $\sigma_{\text{low}}^2 = \mu/100$, $\sigma_{\text{mid}}^2 = \mu/9$, and $\sigma_{\text{high}}^2 = \mu/2.75$. Parameters were restricted to logical values, with $0 \leq k_b, k_p \leq 1$; $r > 0$, and $t \geq 1$. This thresholding did not change the overall mean of any parameter by more than $\pm 3\%$. R0 was calculated as the ratio of founding cells at a given passage relative to the founding cells of the previous passage. Points and error bars (offset to reduce overlap) represent mean values and 95% confidence intervals, and solid lines display best-fit regressions (Table S2).

The low cost of maintaining a biofilm makes it well suited as a potential bet-hedging strategy, increasing the long-term geometric mean fitness in unpredictable environments by minimizing the variance in fitness through time. To test this prediction, we used our model framework to construct a simulated passing regime in which growth and transmission parameters were subjected to differing levels of variance. We assigned inoculum populations of planktonic cells a fixed colonization rate, c (applied relative to r), and then subjected them to alternating periods of growth and transmission. The parameters r , t , k_p , and k_b were drawn from normal distributions with fixed means μ and differing variances σ^2 between treatments. The values of r , t , and c were used to solve equations 3 and 4; proportions k_p and k_b of these new cells were then passed to the next growth phase, as in equation 7. The fitness function defined in equation 8 (effectively a reproductive number, R0 [14]) was used as our fitness metric for these simulations, calculated as the ratio of founding cells in a given passage relative to the number of founding cells in the previous passage. Simulation results are displayed in Fig. 5.

For all treatments, the variance in R0 declines with increasing c , consistent with biofilm colonization functioning as a bet-hedging strategy for bacteria facing unpredictable selection (Fig. 5A). For low and medium degrees of unpredictability, the average R0 declines monotonically with increasing c , reflecting the penalty imposed on fitness by environmental variance (Fig. 5B). Interestingly, under the high-variance treatment, a pronounced hump shape in the average R0 appears (Table S2), indicating that in extremely unpredictable environments, the trade-off between mean fitness and reduced variance in fitness breaks down and biofilm formation is generally beneficial (Fig. 5B). The combination of direct fitness benefits and bet hedging effects lead to maxima in geometric mean R0 at intermediate colonization rates across all variance treatments (Fig. 5C; Table S2).

DISCUSSION

Many groups have used agent-based models to examine the processes and dynamics of biofilm formation (13, 17–20). While these studies benefit from explicit mechanistic foundations, it is not always straightforward to determine the underlying processes influencing the simulated populations. In this work, we constructed an analytical metapopulation model of allocation between coupled biofilm and planktonic compartments within a growing bacterial population, which allowed us to investigate the

underlying population dynamics in detail. Within the biofilm, cell division limited by geometry and nutrient diffusion rendered its effects inconsequential to the dynamics of the population as a whole, relative to the exponentially expanding pool of planktonic cells. Under inhospitable conditions, in which the population experienced restricted growth and/or frequent disruption, trade-offs between the biofilm and planktonic compartments forced lineages to specialize in whichever fraction was favored for transmission between patches. When conditions become more permissive, the lineage is able to leverage exponential planktonic growth to maintain robust populations in both compartments and at a fraction of the cellular cost of direct biofilm allocation (i.e., at reduced colonization rates c); in general, such cost-saving measures are likely to be favored in any cooperative trait during periods of growth (21). Because maintenance of a biofilm comes at little cost under conditions favoring planktonic growth, biofilm is able to function as a robust and cost-effective hedge against unpredictable environmental change. Conversely, the planktonic fraction is a useful amplifier of biofilm cells even when biofilm is the transmissible propagule—this growth/transmission division of labor is more obvious for strictly nongrowing phenotypes (e.g., spores), but the same logic holds for slow growth in biofilms as well.

We focus primarily on biofilm-planktonic cell populations as a model of survival-fecundity alternate states and therefore use the language of colonization (of biofilms by planktonic cells) and dispersal (from the biofilm) to represent the processes of switching between the two phenotypes. However, the model logic applies to other classes of resistant cells as well, such as persisters and spores. Indeed, there are instances where biofilm formation functions as a prerequisite or amplifying step in the formation of other types of resistant cells; persister cells are often enriched in biofilms (8, 22–25), and biofilm formation is a prerequisite step in fruiting body formation (the preferred site of sporulation) in *Bacillus subtilis* (26, 27); it would be interesting to investigate how investment would be optimized with multiple survival phenotypes available in both simultaneous and sequential contexts. However, the generality of our models with respect to the specifics of a resistant cell type comes at the expense of mechanistic understanding. For example, we assume that resistant cells are continuously produced by vegetative cells; while this mechanism holds for persister cells, which by definition have no or extremely limited growth, it may not hold for established biofilms, where subsequent colonization by clonal planktonic cells can be blocked by extracellular matrix components (28), though the generality of this effect is not well studied. In our models and experiments, we primarily consider nascent populations and high-disturbance regimes and therefore reason that such exclusion would not have major impacts on our results but concede that such effects are likely to play a larger role in the long-term dynamics of the system. Further work to elucidate the mechanistic details of biofilm growth and attachment in similar experimental contexts would help to improve our understanding of how the colonization rate relates to biofilm accumulation as a function of time and population density.

Given the costs inherent to cellular investment in a growth-limited state, one may expect lineages to evolve the ability to efficiently switch between biofilm and planktonic phenotypes, thereby optimizing fitness by reducing lag times and minimizing unnecessary death in the event of environmental disturbance, and indeed, such systems appear to be abundant in nature (29–34). However, we note that environmental sensing in this case would not supplant the need to maintain some level of biofilm as a hedge (Fig. 4 and 5) but rather enhance the efficiency of such maintenance; in environments where catastrophic disturbances occur even at very low frequency, lineages that maintain biofilm regardless will still have better chances of survival. One would therefore predict biofilm to be completely lost in only the most constant environments.

Another likely outcome of long-term selection in environments that provide distinct spatial niches is genetic and morphological diversification within the population, resulting in coexisting lineages specialized to a particular niche (15, 16, 35, 36) that may or may not display similar division of labor between types. Such diversity can evolve

rapidly but generally relies on the systems remaining undisturbed for at least several days (15, 35, 36); we speculate that this is due to saturation of readily available niches and thus increased selective pressure toward exploitation of any remaining sites within the environment. In experimental systems involving repeated dilutions similar to those presented here (16), diversity was slower to emerge, with smooth-colony variants appearing within 150 generations and more rugose variants only after 300 to 400 generations. Given that our experiments involved slower growth, more frequent dilutions, and fewer total passages, it is perhaps unsurprising that diversity would be slower to emerge (Fig. S3). Our models and experiments therefore suggest that microbial populations can enjoy the benefits of dividing labor between phenotypes within a single genotype and indeed may be at an advantage when the environment changes unpredictably (Fig. 5).

Phenotypic regulation to further optimize allocation between biofilm and planktonic lifestyles would help expedite the evolution of rudimentary life cycles at the population level, alternating between a growing “soma” and dispersive “propagules” with distinct demographics associated with each phase. Under the formalism presented here, either the biofilm or the planktonic compartment alone, or some combination thereof, may serve as dispersing propagules. The historical archetype has generally held that the biofilm functions as the soma, with motile planktonic cells as dispersive propagules (37–39). More recently, Hammerschmidt et al. (40) found that alternating selection on dispersive and biofilm phenotypes in *Pseudomonas fluorescens* leads to the evolution of a lifestyle in which cooperative biofilm cells producing shared adhesive molecules form a pellicle that functions as the growing soma, and planktonic nonadhesive cheats are coopted as dispersive propagules, thereby dividing labor between the two cellular fractions and increasing the overall fitness of the lineage. Our results indicate that the opposite cycle (biofilm cells as propagules, planktonic cells as soma) could also be viable, as the population can still reap the benefits of dividing labor between specialized cellular fractions. Indeed, where individual patches are permissive to growth but transmission between patches is exceedingly harsh (e.g., wind or animal dispersal), dispersal via biofilm aggregates and growth within a planktonic “soma” would offer the greatest advantage, as the “soma” would accumulate biomass rapidly, and dispersal propagules would enjoy increased survival at little reproductive cost given the hostile transmission conditions. For example, biofilm formation and other survival phenotypes are likely important to successful transmission via fomites, upon which bacteria can remain viable for months (41). Dispersal in physically linked groups (i.e., budding dispersal [42]) may also help maintain cooperative traits or competitive advantages (43), thereby potentially accelerating colonization when a new patch is reached. The biofilm “streamers” observed by Drescher et al. (44) may be another example of this mode of transmission, where flow rates are such that the biofilm forms physical bridges to allow colonization of vacant surfaces in a topographically complex environment, as full detachment would prevent recolonization of adjacent surfaces because of extreme shear forces.

Taken together, our results highlight the evolutionary significance of within-population phenotypic heterogeneity and its consequences for survival and fecundity in mixed-transmission environments. By optimizing the switching rate between robust and fecund specialists (here, the colonization rate from the planktonic to the biofilm fraction, though we note that other mechanisms could lead to equivalent outcomes, such as the steady-state frequencies of genotypes arising from within-population diversification, as in references 16 and 36), lineages were able to maximize fitness and transmission across a wide range of environments, as well as enhance survival in the face of catastrophic changes within the environment. The rate of phenotypic switching is therefore an essential parameter upon which selection may act when multiple phenotypes can persist within lineages.

MATERIALS AND METHODS

Passaging experiment. A mid-exponential-phase culture of *P. aeruginosa* PAO1 was used to inoculate 200 μ l of LB and one 3-mm sterile glass bead into each of 24 wells of a 96-well plate at an OD of 0.05. Plates were sealed with AeraSeal tape, and cultures were grown statically at 24°C in a humidified chamber. Every 12 h (growth conditions were chosen to prevent entry into stationary phase, where

multiple regulatory systems that modulate biofilm and growth behaviors are engaged), biofilm allocation was measured by removing the liquid phase and measuring the OD, washing the attached biofilm with sterile water, resuspending it by vortexing it for 15 min in 200 μ l of fresh LB, and then measuring the OD of the resuspended biofilm cells. Twelve lines had only the planktonic cells passaged, while the other 12 had only biofilm cells passaged; in each case, cells were diluted to an inoculum OD of 0.05 and 20 passages were performed. To assess whether morphological diversification has occurred under biofilm selection, aliquots from frozen stocks of three lineages were spread onto LB plates and morphology was assessed after incubation for 48 h at room temperature. Individual clones from each population were also selected and assayed for population allocation as described above.

Statistics and mathematical analysis. Agent-based simulations were performed with iDynaMiCs (13), and analyses were performed with Mathematica. Numerical modeling (45) and statistics were performed in R (46), unless otherwise noted.

SUPPLEMENTAL MATERIAL

Supplemental material for this article may be found at <https://doi.org/10.1128/mBio.00672-17>.

TEXT S1, PDF file, 0.5 MB.

TEXT S2, PDF file, 0.5 MB.

TEXT S3, PDF file, 0.5 MB.

FIG S1, PDF file, 0.1 MB.

FIG S2, PDF file, 0.1 MB.

FIG S3, PDF file, 0.1 MB.

TABLE S1, PDF file, 0.4 MB.

TABLE S2, PDF file, 0.4 MB.

ACKNOWLEDGMENTS

We thank R. Parthasarathy, B. Bohannon, and members of the Brown laboratory for helpful comments.

We have no conflicts of interest to declare.

N.V.L. was supported by a scholarship from the School of the Biological Sciences, University of Edinburgh. L.M. was supported by Wellcome Trust grant WT095831. W.C.R. was supported by a Packard Foundation fellowship. L.M. and S.P.B. were supported by HSPF grant RGP0011/2014. The funders had no role in study design, data collection and interpretation, or the decision to submit the work for publication.

REFERENCES

1. Stearns SC. 1992. The evolution of life histories. Oxford University Press, Bethesda, MD.
2. De Paepe M, Taddei F. 2006. Viruses' life history: towards a mechanistic basis of a trade-off between survival and reproduction among phages. *PLoS Biol* 4:e193. <https://doi.org/10.1371/journal.pbio.0040193>.
3. Heineman RH, Brown SP. 2012. Experimental evolution of a bacteriophage virus reveals the trajectory of adaptation across a fecundity/longevity trade-off. *PLoS One* 7:e46322. <https://doi.org/10.1371/journal.pone.0046322>.
4. Gudelj I, Weitz JS, Ferenci T, Claire Horner-Devine M, Marx CJ, Meyer JR, Forde SE. 2010. An integrative approach to understanding microbial diversity: from intracellular mechanisms to community structure. *Ecol Lett* 13:1073–1084. <https://doi.org/10.1111/j.1461-0248.2010.01507.x>.
5. Green JL, Bohannon BJM, Whitaker RJ. 2008. Microbial biogeography: from taxonomy to traits. *Science* 320:1039–1043. <https://doi.org/10.1126/science.1153475>.
6. Cano RJ, Borucki MK. 1995. Revival and identification of bacterial spores in 25- to 40-million-year-old Dominican amber. *Science* 268:1060–1064. <https://doi.org/10.1126/science.7538699>.
7. Vreeland RH, Rosenzweig WD, Powers DW. 2000. Isolation of a 250 million-year-old halotolerant bacterium from a primary salt crystal. *Nature* 407:897–900. <https://doi.org/10.1038/35038060>.
8. Lewis K. 2010. Persister cells. *Annu Rev Microbiol* 64:357–372. <https://doi.org/10.1146/annurev.micro.112408.134306>.
9. Wood TK, Knabel SJ, Kwan BW. 2013. Bacterial persister cell formation and dormancy. *Appl Environ Microbiol* 79:7116–7121. <https://doi.org/10.1128/AEM.02636-13>.
10. Van Acker H, Van Dijck P, Coenye T. 2014. Molecular mechanisms of antimicrobial tolerance and resistance in bacterial and fungal biofilms. *Trends Microbiol* 22:326–333. <https://doi.org/10.1016/j.tim.2014.02.001>.
11. Werner E, Roe F, Bugnicourt A, Franklin MJ, Heydorn A, Molin S, Pitts B, Stewart PS. 2004. Stratified growth in *Pseudomonas aeruginosa* biofilms. *Appl Environ Microbiol* 70:6188–6196. <https://doi.org/10.1128/AEM.70.10.6188-6196.2004>.
12. Fux CA, Costerton JW, Stewart PS, Stoodley P. 2005. Survival strategies of infectious biofilms. *Trends Microbiol* 13:34–40. <https://doi.org/10.1016/j.tim.2004.11.010>.
13. Lardon LA, Merkey BV, Martins S, Dötsch A, Picioreanu C, Kreft JU, Smets BF. 2011. iDynaMiCs: next-generation individual-based modelling of biofilms. *Environ Microbiol* 13:2416–2434. <https://doi.org/10.1111/j.1462-2920.2011.02414.x>.
14. Frank SA. 1996. Models of parasite virulence. *Q Rev Biol* 71:37–78. <https://doi.org/10.1086/419267>.
15. Rainey PB, Travisano M. 1998. Adaptive radiation in a heterogeneous environment. *Nature* 394:69–72. <https://doi.org/10.1038/27900>.
16. Poltak SR, Cooper VS. 2011. Ecological succession in long-term experimentally evolved biofilms produces synergistic communities. *ISME J* 5:369–378. <https://doi.org/10.1038/ismej.2010.136>.
17. Hellweger FL, Clegg RJ, Clark JR, Plugge CM, Kreft JU. 2016. Advancing microbial sciences by individual-based modelling. *Nat Rev Microbiol* 14:461–471. <https://doi.org/10.1038/nrmicro.2016.62>.
18. Kreft JU. 2004. Biofilms promote altruism. *Microbiology* 150:2751–2760. <https://doi.org/10.1099/mic.0.26829-0>.
19. Momeni B, Waite AJ, Shou W. 2013. Spatial self-organization favors heterotypic cooperation over cheating. *eLife* 2:e00960. <https://doi.org/10.7554/eLife.00960>.
20. van Gestel J, Nowak MA. 2016. Phenotypic heterogeneity and the evolution of

- lution of bacterial life cycles. *PLoS Comput Biol* 12:e1004764. <https://doi.org/10.1371/journal.pcbi.1004764>.
21. Cornforth DM, Sumpter DJT, Brown SP, Brännström Å. 2012. Synergy and group size in microbial cooperation. *Am Nat* 180:296–305. <https://doi.org/10.1086/667193>.
 22. Singh R, Ray P, Das A, Sharma M. 2009. Role of persisters and small-colony variants in antibiotic resistance of planktonic and biofilm-associated *Staphylococcus aureus*: an in vitro study. *J Med Microbiol* 58:1067–1073. <https://doi.org/10.1099/jmm.0.009720-0>.
 23. Nadell CD, Xavier JB, Foster KR. 2009. The sociobiology of biofilms. *FEMS Microbiol Rev* 33:206–224. <https://doi.org/10.1111/j.1574-6976.2008.00150.x>.
 24. Haaber J, Cohn MT, Frees D, Andersen TJ, Ingmer H. 2012. Planktonic aggregates of *Staphylococcus aureus* protect against common antibiotics. *PLoS One* 7:e41075. <https://doi.org/10.1371/journal.pone.0041075>.
 25. Høiby N, Bjarnsholt T, Givskov M, Molin S, Ciofu O. 2010. Antibiotic resistance of bacterial biofilms. *Int J Antimicrob Agents* 35:322–332. <https://doi.org/10.1016/j.ijantimicag.2009.12.011>.
 26. Branda SS, González-Pastor JE, Ben-Yehuda S, Losick R, Kolter R. 2001. Fruiting body formation by *Bacillus subtilis*. *Proc Natl Acad Sci U S A* 98:11621–11626. <https://doi.org/10.1073/pnas.191384198>.
 27. Aguilar C, Vlamakis H, Guzman A, Losick R, Kolter R, Eichenberger P. 2010. KinD is a checkpoint protein linking spore formation to extracellular matrix production in *Bacillus subtilis*. *mBio* 1:e00035-10. <https://doi.org/10.1128/mBio.00035-10>.
 28. Nadell CD, Drescher K, Wingreen NS, Bassler BL. 2015. Extracellular matrix structure governs invasion resistance in bacterial biofilms. *ISME J* 9:1700–1709. <https://doi.org/10.1038/ismej.2014.246>.
 29. Schuster M, Sexton DJ, Diggle SP, Greenberg EP. 2013. Acyl-homoserine lactone quorum sensing: from evolution to application. *Annu Rev Microbiol* 67:43–63. <https://doi.org/10.1146/annurev-micro-092412-155635>.
 30. Cornforth DM, Papat R, McNally L, Gurney J, Scott-Phillips TC, Ivens A, Diggle SP, Brown SP. 2014. Combinatorial quorum sensing allows bacteria to resolve their social and physical environment. *Proc Natl Acad Sci U S A* 111:4280–4284. <https://doi.org/10.1073/pnas.1319175111>.
 31. Barraud N, Schleheck D, Klebensberger J, Webb JS, Hassett DJ, Rice SA, Kjelleberg S. 2009. Nitric oxide signaling in *Pseudomonas aeruginosa* biofilms mediates phosphodiesterase activity, decreased cyclic di-GMP levels, and enhanced dispersal. *J Bacteriol* 191:7333–7342. <https://doi.org/10.1128/JB.00975-09>.
 32. Huynh TT, McDougald D, Klebensberger J, Al Qarni B, Barraud N, Rice SA, Kjelleberg S, Schleheck D. 2012. Glucose starvation-induced dispersal of *Pseudomonas aeruginosa* biofilms is cAMP and energy dependent. *PLoS One* 7:e42874. <https://doi.org/10.1371/journal.pone.0042874>.
 33. Dow JM, Crossman L, Findlay K, He YQ, Feng JX, Tang JL. 2003. Biofilm dispersal in *Xanthomonas campestris* is controlled by cell-cell signaling and is required for full virulence to plants. *Proc Natl Acad Sci U S A* 100:10995–11000. <https://doi.org/10.1073/pnas.1833360100>.
 34. Sauer K, Cullen MC, Rickard AH, Zeef LA, Davies DG, Gilbert P. 2004. Characterization of nutrient-induced dispersion in *Pseudomonas aeruginosa* PAO1 Biofilm. *J Bacteriol* 186:7312–7326. <https://doi.org/10.1128/JB.186.21.7312-7326.2004>.
 35. Boles BR, Thoendel M, Singh PK. 2004. Self-generated diversity produces “insurance effects” in biofilm communities. *Proc Natl Acad Sci U S A* 101:16630–16635. <https://doi.org/10.1073/pnas.0407460101>.
 36. Kim W, Levy SB, Foster KR. 2016. Rapid radiation in bacteria leads to a division of labour. *Nat Commun* 7:10508. <https://doi.org/10.1038/ncomms10508>.
 37. O’Toole GA, Kaplan HB, Kolter R. 2000. Biofilm formation as microbial development. *Annu Rev Microbiol* 54:49–79. <https://doi.org/10.1146/annurev.micro.54.1.49>.
 38. Sauer K, Camper AK, Ehrlich GD, Costerton JW, Davies DG. 2002. *Pseudomonas aeruginosa* displays multiple phenotypes during development as a biofilm. *J Bacteriol* 184:1140–1154. <https://doi.org/10.1128/jb.184.4.1140-1154.2002>.
 39. Monds RD, O’Toole GA. 2009. The developmental model of microbial biofilms: ten years of a paradigm up for review. *Trends Microbiol* 17:73–87. <https://doi.org/10.1016/j.tim.2008.11.001>.
 40. Hammerschmidt K, Rose CJ, Kerr B, Rainey PB. 2014. Life cycles, fitness decoupling and the evolution of multicellularity. *Nature* 515:75–79. <https://doi.org/10.1038/nature13884>.
 41. Kramer A, Schwebke I, Kampf G. 2006. How long do nosocomial pathogens persist on inanimate surfaces? A systematic review. *BMC Infect Dis* 6:130. <https://doi.org/10.1186/1471-2334-6-130>.
 42. Kümmerli R, Gardner A, West SA, Griffin AS. 2009. Limited dispersal, budding dispersal, and cooperation: an experimental study. *Evolution* 63:939–949. <https://doi.org/10.1111/j.1558-5646.2008.00548.x>.
 43. Kragh KN, Hutchison JB, Melaugh G, Rodesney C, Roberts AEL, Irie Y, Jensen PØ, Diggle SP, Allen RJ, Gordon V, Bjarnsholt T. 2016. Role of multicellular aggregates in biofilm formation. *mBio* 7:e00237-16. <https://doi.org/10.1128/mBio.00237-16>.
 44. Drescher K, Shen Y, Bassler BL, Stone HA. 2013. Biofilm streamers cause catastrophic disruption of flow with consequences for environmental and medical systems. *Proc Natl Acad Sci U S A* 110:4345–4350. <https://doi.org/10.1073/pnas.1300321110>.
 45. Soetaert K, Petzoldt T, Setzer RW. 2010. Solving differential equations in R: package deSolve. *J Stat Softw* 33:1–25. http://www.academia.edu/13415757/Solving_differential_equations_in_R_Package_deSolve.
 46. R Core Team. 2015. R: a language and environment for statistical computing. R Foundation for Statistical Computing, Vienna, Austria.
 47. Akaike H. 1981. Likelihood of a model and information criteria. *J Econom* 16:3–14. [https://doi.org/10.1016/0304-4076\(81\)90071-3](https://doi.org/10.1016/0304-4076(81)90071-3).